

Control of Separation For NACA 2412 Airfoil At Different Angles of Attack Using Air Blowing

Dr. Jalal M. Jalil¹ Dr. Assim H. Yousif^{2*}
& Yasser Ahmed Mahmood^{3*}

Received on: 17/11/2009

Accepted on: 3/6/2010

Abstract

The study of the separation control using the jet blowing based on the computation of Reynolds-average Navier-Stocks equations is carried out in this work. A numerical model based on collocated Finite Volume Method is developed to solve the governing equations on a body-fitted grid, to compute the performance of airfoil by using the blowing jet. Above of all, the performance of turbulence model is investigation. A revised $k\omega$ model is proposed as the known turbulence models perform well in reproducing the flow of airfoil at pre-stall or stall angle of attack. The systematical investigation of the jet blowing is conducted on the NACA 2412 airfoil in the range of attack angle from 0° to 30° included up and beyond the stall angle at range of $Re=3.4 \times 10^5 - 1.7 \times 10^6$. The influence of some parameters associated with using jet blowing, such as its location, and the speed ratio (U_j/U) strength on the performance of the NACA 2412 airfoil has also been studied. The result shows that the jet blowing is effective in controlling the separation at $0.3C$ and $U_j/U=2$. The large separation regions cannot be completely removed by the jet blowing. However, the flow structure can be regularized. The lift coefficient of the control airfoil is also increased with the angle of the attack. The experimental results are obtained on airfoil NACA 2412 at $0.3C$ blowing and $U_j/U=2$, the results are been good agreement with the computational results.

Keywords: Control separation, angle of attack, Air blowing, CFD.

السيطرة على الانفصال لمقطع جناح (NACA 2412) لمختلف زوايا الهجوم باستخدام نفخ الهواء

الخلاصة

تم في هذا البحث تقديم دراسة عددية للتكهن بألية السيطرة و التحكم بجريان الهواء وباستخدام الدفع، حيث تم بناء نموذج رياضي يعتمد الحل العددي لمعادلات نافير-ستوك (Navier-Stock) وباستخدام طريقة الحجوم المحددة (Finite Volume Method) ذات الترتيب (Collocated) المبنية على نظام الاحداثيات غير المتعامدة للشبكة المتولدة، لحساب اداء المطيار المجهز بألية سيطرة (عملية الدفع) على جريان الهواء المار حوله. اجريت دراسة لمعرفة أداء بعض نماذج الاضطراب، حيث ان الانموذج الاضطرابي القياسي ($k-\omega$) يعتبر من النماذج الاضطرابية الواسعة الانتشار التي تمتاز بقوة ادائها تجاه تحليل جريان المائع حول المطيار عند او قبل الوصول الى زاوية الانهواء (Stall Angle). اجريت دراسة حسابية على مقطع المطيار NACA 2412

*Electromechanical Engineering Department, University of Technology/ Baghdad

**Mechanical Engineering Department, University of Technology/ Baghdad

بوجود الية السيطرة (عملية الدفع) ولزوايا هجوم من 0° الى 30° تتضمن زاوية الانهواء عند عدد رينولدز من 3.4×10^5 الى 1.7×10^6 , حيث تمت دراسة مختلف المتغيرات ونسبة سرعة الدفع الى سرعة الهواء الحر (U_j/U) على اداء المظيار NACA 2412 . بينت النتائج المستحصلة ان وجود تأثير عملية الدفع كألية سيطرة يكون فعالا في السيطرة على عملية الانفصال و خاصة عند $0.3C$ و $U_j/U=2$. حيث ان مناطق الانفصال الكبيرة لا يمكن ازالتها بصورة نهائية, الا ان شكل الجريان يكون اكثر انتظاما . كما ان معامل الرفع يمكن ان يزداد بزيادة زوايا الهجوم والذخم المتولد من زيادة سرعة الدفع نسبة الى سرعة الهواء الحر . تبين ان النتائج العملية المستحصلة حول المظيار NACA 2412 عند $0.3C$ و $U_j/U=2$ ذات توافق جيد مع النتائج النظرية.

Introduction

Active manipulation of separated flows over lifting surfaces remains to be highly interesting because of its potential application in many fields. There are manifold measures to control the separation based on concepts from boundary layer to coherent structure and from single jet blowing. This method is developed by various researchers; (e.g. Ravindran [1], a numerical study is performed to investigate the effects of unsteady blowing on airfoils, the unsteady blowing is introduced at leading edge of the airfoil in the form of tangential jet. John and Keith [2], describes experiments aimed demonstrating the effectiveness of pulsed vortex generator jets in controlling separation on aircraft wings. Huang L. and Huang P. [3], the design parameter of a two-jet system of blowing jet, a real-coded EARED genetic algorithm is built on top of the CFD code, guiding the movement of a blowing jet along the airfoil's upper surface. Zhuo Wang and Bernd Stoffel [4], active control with single synthetic jet on an NACA63₃-018 airfoil at stall angle of attack is investigate numerically using Reynolds-averaged Navier-Stokes (RANS) equations with a

revised k- model. Mustafa [5], a laminar separation bubble formation and its control with jet blowing over NACA2415 airfoil are numerically studied, it is shown that when the blowing jet is placed before bubble and center of bubble, the separation bubble over the airfoil is eliminated and increasing aerodynamic performance. Instead of usually used k- turbulent model, the k- ω was used originally introduced by Saffman 1982 but popularized by Wilcox [6]. In this model, use is made of an equation for an inverse time scale ω . It will solve two-dimensional turbulent flow over airfoil NACA 2412 with different angles of attack using k- ω turbulent model and collocated grids. The main objectives at this work is to investigate the stalling conditional (separation point) on airfoil of NACA 2412 and how it can be delayed or reduced by jet blowing at different Reynolds numbers ($Re=3.4 \times 10^5$ - 1.7×10^6) and angles of attack (0° to 30° included up and beyond the stall angle), based on the computation of Reynolds average Navier-Stocks equations, A numerical model based on collocated Finite Volume method is developed to solve the governing equations on a body-fitted grid, influence of jet

blowing location on the upper surface of the airfoil on the aerodynamic characteristic of airfoil, influence of speed jet ratio on the aerodynamic characteristic of airfoil.

An experimental investigation has been done to validate the numerical approach of the boundary-layer separation phenomenon on the airfoil model (NACA 2412). This model was tested in the low speed wind tunnel. The use of mass transfer such as air blowing through jet holes located at the pressure side of the model was used to prevent or delay the flow separation.

Reynolds-Averaged Navier-Stokes Equations

In this section, we will summarize the basic equations governing fluid flow in turbulent, steady, incompressible flows. The derivation of these equations, details regarding the constitutive relations used and the various turbulence modeling assumptions employed can be found in several sources (e.g. White [7], Ferziger and Peric [8]). Employing indicial notation, the instantaneous form of continuity and momentum equations in cartesian coordinates can be written as follows:

$$\frac{\partial}{\partial x_j} (u_j) = 0 \quad \dots(1)$$

$$\frac{\partial}{\partial x_j} (r u_j u_i) = -\frac{\partial p}{\partial x_i} + \frac{\partial t_{ij}}{\partial x_j} \mathbf{M} \quad \dots(2)$$

C_m	C_1	C_2	S_k	S_e	a^*	b^*
0.09	1.44	1.92	1.0	1.3	0.56	- 0.075

$$t_{ij} = m \left(\frac{\partial u_i}{\partial x_j} + \frac{\partial u_j}{\partial x_i} \right) - \frac{2}{3} m \frac{\partial u_i}{\partial x_j} . d_{ij} \quad \dots(3)$$

Two-equation model is the k- ω model, which will be presented here in the form given by Wilcox [6]:

$$\frac{\partial (r u_j f)}{\partial x_j} = \frac{\partial}{\partial x_j} \left[\left(m + \frac{m}{S_f} \right) \frac{\partial f}{\partial x_j} \right] + R_1 + R_2 \quad \dots [4]$$

or with: $f \equiv k, e$ and w

Where for the k-eqn.

for the ϵ -eqn. for the w -eqn

$$R_i = \begin{cases} \Pi & \dots\dots [5] \\ \frac{C_1 e \Pi}{k} \\ \frac{a^* w \Pi}{k} \end{cases}$$

$$R_i = \begin{cases} -r e = \frac{C_m r^3 k^2}{m} \\ -C_2 r \frac{e^2}{k} \\ -b^* r w^2 \end{cases} \quad \dots\dots [6]$$

The various constants used in the standard model have the following values:

**General Differential Form of the
Transport Equations:**

The conservative form of all fluid transport equations, including equations for scalar quantities (k, ω, ϵ) can usefully be cast in one general form as shown below.

$$\int_s r f \bar{u} \cdot \bar{n} ds = \int_s \Gamma_f \text{grad} f \cdot \bar{n} ds + \int_\Omega S_f d\Omega$$

..... [7]

The term on the left hand side is the convective term, the first term on the right hand side is the diffusive term, and the last term is the source term. The source term includes both the source of and any other terms that cannot find a place in any of the convection or diffusion terms.

The full discretization of the transport equation on a non-orthogonal mesh can now be given. By approximating the convective fluxes with the central difference scheme, the steady transport equation can be discretized as:

$$A f + B f = c$$

..... [8]

For a discretization of the two-dimensional transport equation the individual coefficients of the A, B and c arrays are, the mesh is shown in figure (1)

$$a_E = -G_e^{11} + \frac{1}{2} r \bar{u}_e$$

$$a_W = G_w^{11} - \frac{1}{2} r \bar{u}_w$$

$$a_N = -G_n^{22} + \frac{1}{2} r \bar{u}_n$$

$$a_S = -G_s^{22} - \frac{1}{2} r \bar{u}_s$$

$$a_P = -(a_E + a_W + a_N + a_S) + (r \bar{u}_e - r \bar{u}_w + r \bar{u}_n - r \bar{u}_s)$$

$$c = S_P \Omega$$

$$b_E = \frac{1}{4} (G_n^{21} - G_s^{21})$$

$$b_W = -\frac{1}{4} (G_n^{21} - G_s^{21})$$

$$b_N = \frac{1}{4} (G_e^{12} - G_w^{12})$$

$$b_S = -\frac{1}{4} (G_e^{12} - G_w^{12})$$

$$b_P = 0$$

$$b_{NE} = \frac{1}{4} (G_e^{12} + G_n^{21})$$

$$b_{NW} = -\frac{1}{4} (G_w^{12} + G_n^{21})$$

$$b_{SE} = -\frac{1}{4} (G_e^{12} + G_s^{21})$$

$$b_{SW} = \frac{1}{4} (G_w^{12} + G_s^{21})$$

..... [9]

**The pressure Gradient Term for
source term:**

$$P = -\frac{1}{2} (A_e^{11} P_E + A_w^{11} P_W + A_n^{22} P_N + A_s^{22} P_S)$$

..... [10]

The pressure Correction

Equation:

$$\frac{r A_e^{11}}{a_{pe}} \left[(A_e^{11} P'_E - A_e^{11} P'_P) + \frac{1}{4} (A_e^{22} P'_N - A_s^{22} P'_S) \right] -$$

$$\frac{r A_w^{11}}{a_{pw}} \left[(A_w^{11} P'_P - A_w^{11} P'_W) + \frac{1}{4} (A_w^{22} P'_N - A_s^{22} P'_S) \right] +$$

$$\frac{r A_n^{11}}{a_{pn}} \left[(A_n^{22} P'_N - A_n^{22} P'_P) + \frac{1}{4} (A_n^{11} P'_E + A_w^{11} P'_W) \right] -$$

$$\frac{rA_s^{11}}{a_{ps}} \left[(A_s^{22} P'_p - A_s^{22} P'_s) + \frac{1}{4} (A_s^{11} P'_E - A_w^{11} P'_W) \right] = S_M$$

..... [11]

S_M : The mass flux source term

Experimental work:

An experimental investigation has been done to validate the numerical approach of the boundary-layer separation phenomenon on the airfoil model (NACA 2412) Fig. (2). It was a cambered airfoil of constant chord and made of laminated wood. The airfoil aspect ratio of 2.2, span and chord were 33 and 15 cm. respectively and the thickness to chord ratio was 0.12. This model was tested in the low speed wind tunnel of $Re=3.4*10^5$ Fig. (3). It was made to span the test-section of the wind tunnel, care being taken to seal the airfoil tips to the side walls of the tunnel and to achieve any incidence angle (α) of airfoil. The leading and trailing edges of the airfoil were made to form a circular arc. Row of four blowing holes in the span wise direction were located on the upper surface of the airfoil. Each hole had 1.5 mm diameter with angle like incidence and the span wise distance is 10 cm between any two neighboring holes. The row of holes is located in span wise direction at $(x/c) = 0.3$ from the airfoil leading edge. The holes geometry dimensions and located were taken as recommended by Ref. [9], and the holes were made to provide a blowing air. The model surface was coated with "cellar" resin against the absorption of oil which was used for flow visualization. In addition all surfaces were painted with a matt-black finish. Also a telly-surface

measurement was made to assess the smoothness of the surfaces which were smoothed to avoid a slight roughness that might influence boundary-layer transition.

The method used to determine the separation position was the oil film technique, mixture of oil, (63% kerosene and 37% Paraffin), and this method was adopted to determine the separation position.

Result and Discussion:

Figures (4(a,b)) Shows the photos obtained from the experimental test. These two photos show clearly the luck of using the oil film technique for the two cases with and without blowing. The main point arised from these photos is that the experimental set up techniques and facilities gave acceptable results.

The experimental and computational results are obtained on airfoil at 0.3C blowing, $U_j/U=2$ and $Re=3.4*10^5$ in table (1), the results are been good agreement between them. The differences between the experiment and numerical simulation results over the NACA airfoil can also be attributed to other factors and errors which exist both on the experimental side and the numerical simulation side. On the experimental side, error in airfoil model, installation disturbance of measurement devices, interference between wind-tunnel wall and airfoil body, and free-stream turbulence and boundary-layer trip effects can create errors in the measurements. On the numerical simulation side, turbulence models, grid density, and the limitations of two-dimensional simulation can produce computational inaccuracies.

For the NACA 2412 and $Re=1.7 \times 10^6$ at different blowing position as shown in Fig. (5, 6, 7, 8), and blowing at $\alpha = 10$, it seen that at blowing point (0.1C) the α_{max} is larger than the other (increase from $\alpha = 14$ to $\alpha = 24$ at $U_j/U = 10$), and when increase the U_j/U at the same position of blowing the C_{Lmax} and α_{max} increase.

As shown in Fig. (9), the perfect jet ratio is equal two when effect it on the $(C_L/C_D)_{max}$, because when increase the jet ratio the drag coefficient increase because the skin friction increase.

In Fig. (10) five different jet blowing ($U_j/U=1, 2, 3, 4, 5$) at $\alpha=14$, and compare it with the baseline (without blowing). When jet blowing applied near and before the separation position (50% of chord), the separation is most effectively delayed and hence the separation bubble and circulation are much smaller than the other cases (at $U_j/U=2$).

Conclusions

1- Navier-Stokes simulations are necessary for the flow control airfoils studies due to the complexity of the flow field and the strong viscous effects. The results indicate that this approach is an efficient and accurate way of modeling control airfoils with jet blowing.

2- The jet blowing technology is a useful way of achieving very high lift at even zero angle of attack. It can also eliminate the vortex shedding in the trailing edge region, which is a potential noise source. The jet blowing as the flow control device is effective in controlling the stalled airfoil flow. The large separation region on stalled airfoil cannot be completely removed by the blowing, but instantaneous

reattachment is possible. The stalled airfoil flow is sensitive to blowing jet ration (U_j/U) and its location, the best at the $U_j/U=2$ and $0.3C$

References

- [1] **Ravindran S.S.** ((Active Control of flow separation over an airfoil)), NASA/TM-1999-209838, 1999.
- [2] **John C. Magill and Keith R. McManus,** ((Exploring the Feasibility of pulsed Jet Separation control for aircraft configurations)), Journal of aircraft 38(1), 48-56, 2001.
- [3] **Huang L., Le Beau R. P. And Huang P. G.,** ((Optimization of blowing and suction control on NACA 0012 airfoil generic algorithm)), Utah state University, Logan, Utah 84322-4130, 2004.
- [4] **Zhuo Wang and Bernd Stoffel,** ((Behavior of synthetic jet on stalled airfoil flow)), Darmstadt University of Technology, 64287 Darmstadt, Germany, 2003.
- [5] **Mustafa Serdar,** ((Control of low Reynolds number flow over airfoil and investigation of aerodynamic performance)), Erciyes University, Graduate school of natural and applied sciences, Ph.D.Thesis, January 2009.
- [6] **Wilcox, D. C.,** ((Wall Matching, a Rational Alternative to wall Functions)), AIAA paper 89-611, 1989.
- [7] **White, F. M.** ((Viscous fluid flow)) 2nd Ed. McGraw. Hill, New York, 1991.
- [8] **Ferziger, J. H. and Peric, M.,** ((Computational Methods for fluid Dynamics.)) 2nd Edition Springer Berlin 1999.
- [9] **Huang, P.G.,** ((Single Suction/Blowing jet study)) Chapter (4), university of Kentucky, 2005.

Nomenclature

Latin notation

$A_{p,e,w,n,s}$: Area of Cell Faces	m^2
$a_{p,e,w,n,s}$: Coefficients in Discretised Equations	
$b_{p,e,w,n,s}$: Coefficients in Discretised Equations	
C	: Chord Length	m
C_L	: Lift coefficient	
C_D	: Drag coefficient	
m^2/s^2	k : Turbulent kinetic energy	
m	: Mass Flux	kg/s
Re	: Reynolds number	
\hat{n}	: Wall-normal unit vector	
P	: Pressure	N/m^2
S_f	: Linearized Source Term For	
u_i	: Velocity in Tensor Notatio	m/s
\bar{u}	: Mean velocity	m/s
U	: Mean velocity components	m/s
U_j	: Jet blowing velocity	m/s
x_i	: Position Vector in Tensor Notation	m

Greek notation:

α	degree	: Angle of Attack	
d_{ij}	:	Kronecker Symbol	
e	:	Dissipation of Turbulent Kinetic Ener	m^2/s^2
f	:	Variable Vector	
Γ	:	Diffusion Coefficient	
μ	:	Molecular or Dynamic Viscosity	$kg/m.s$
μ_t	:	Turbulent (Eddy) Viscosity	m^2/s
ρ	:	Density	kg/m^3
σ_k, σ_ω	:	Empirical Constant in k And ω Transport Equations	
ω	:	Specific Rate of Dissipation of Turbulent Kinetic Energy	
τ	:	Shear Stress	N/m^2
$\Delta\Omega$:	Volume of The Cell	m^3
G^{ij}	:	Geometric diffusion coefficients	
Π	:	Generation (production) of k	m^2/s^2

Subscript:

x, y	: Cartesian coordinates
e, w, n, s	: Face of control volume
E, W, N, S	: Neighbor nodes of node P
P	: Center of control volume
t	: Turbulent

Superscript:

'	: Correction value
---	--------------------

Abbreviations:

- CFD : Computational fluid dynamics
- NACA : The National Advisory Committee for Aeronautics
- AOA : Angle of attack

degree

Table (1) The comparison between the experimental and computation of the position of separation on NACA 2412

α	Position of separation from leading edge before blowing (experimental) (*C)	Position of separation from leading edge after blowing ($U_j/U=2$) (experimental) (*C)	Position of separation from leading edge before blowing (computational) (*C)	Position of separation from leading edge after blowing ($U_j/U=2$) (computational) (*C)
10	0.9	N0 separation	0.95	N0 separation
14	0.63	0.8	0.65	0.83
16	0.35	0.55	0.4	0.59
20	0.25	0.5	0.3	0.54
24	0.2	0.35	0.25	0.39
30	0.1	0.25	0.15	0.3

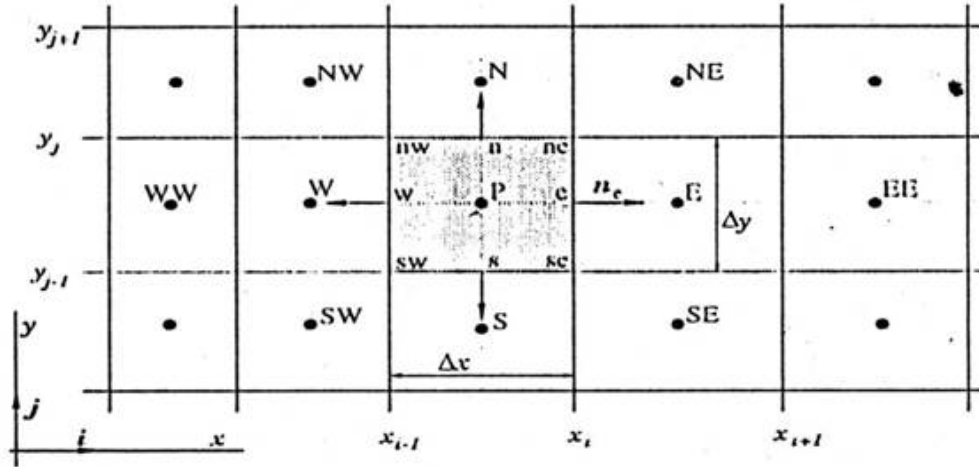


Figure (1) A typical CV and the notation used for a Cartesian 2D grid

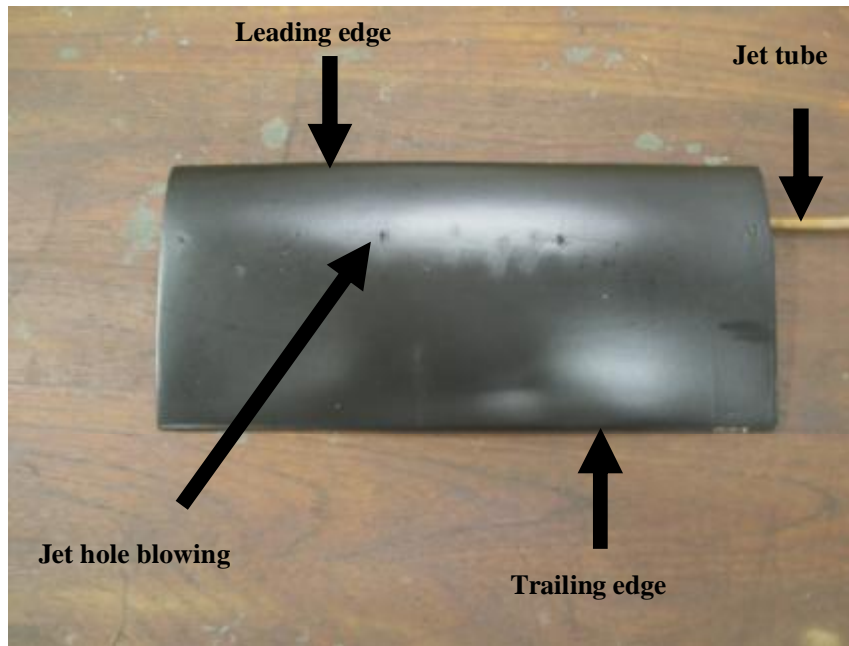


Figure (2) Airfoil of NACA 2412

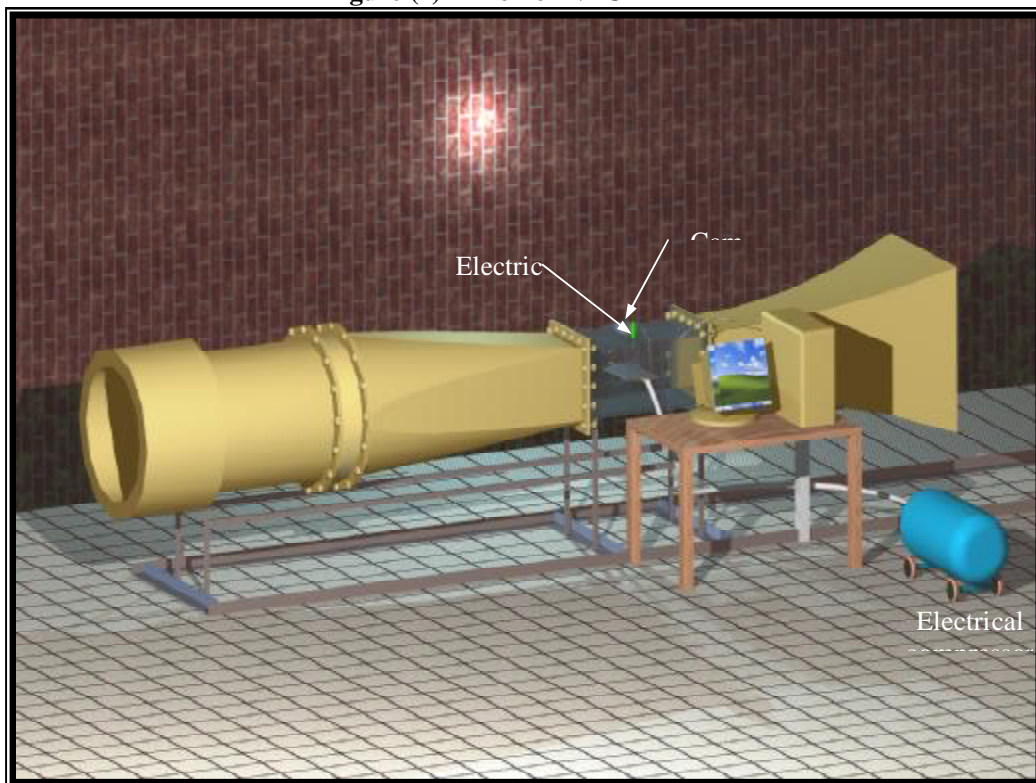
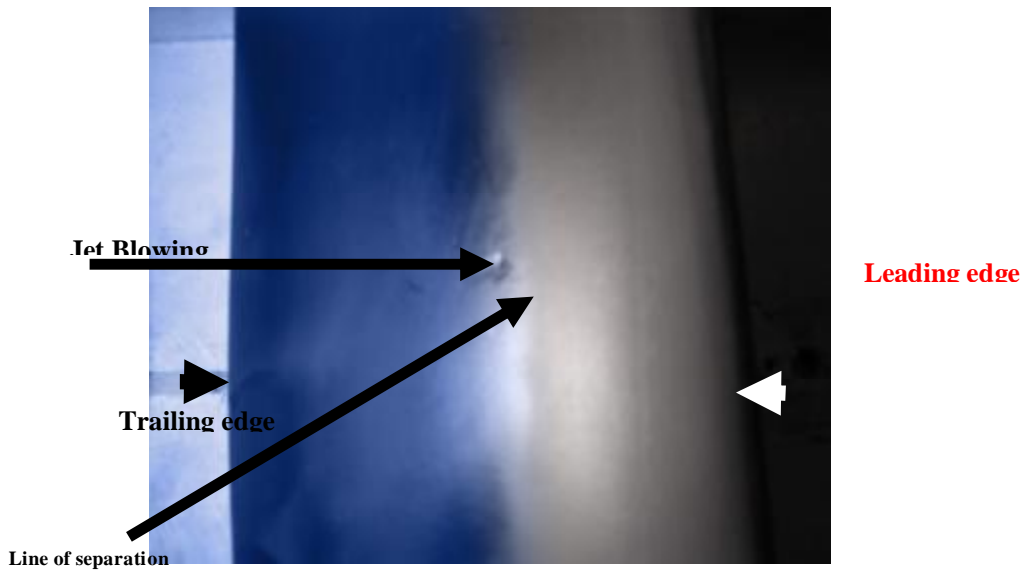
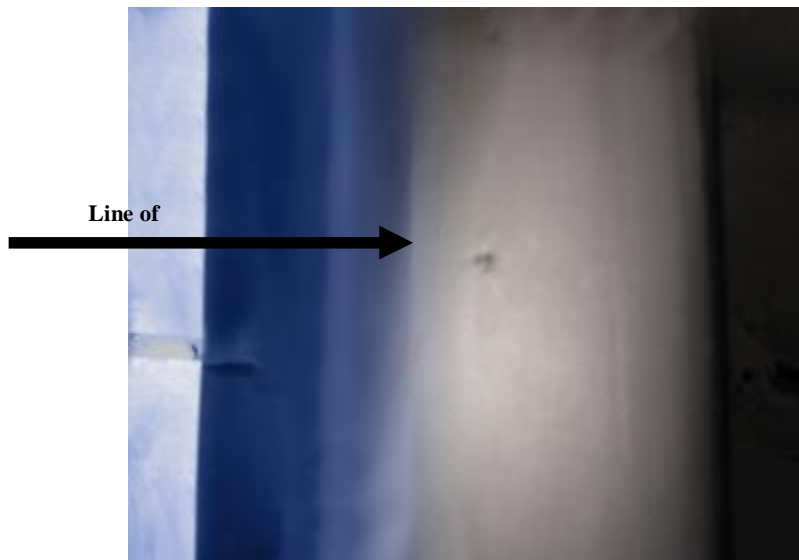


Figure (3) Wind Tunnel



(a) Separation line without blowing at $\alpha = 24$



(b) Separation line with blowing at $\alpha = 24$

Figure (4)

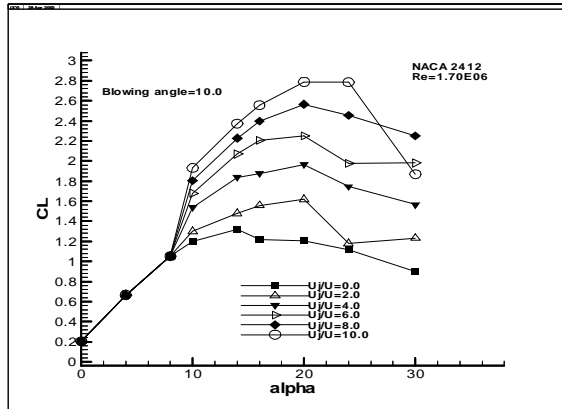


Figure (5) Lift coefficient vs. alpha at blowing position (0.1C)

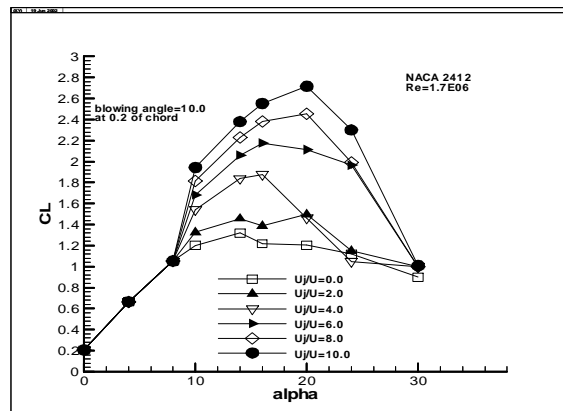


Figure (6) Lift coefficient vs. alpha at blowing Position (0.2C)

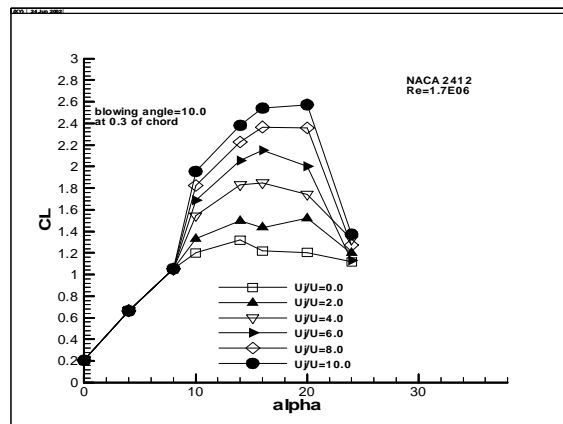


Figure (7) Lift coefficient vs. alpha at blowing position (0.3C)

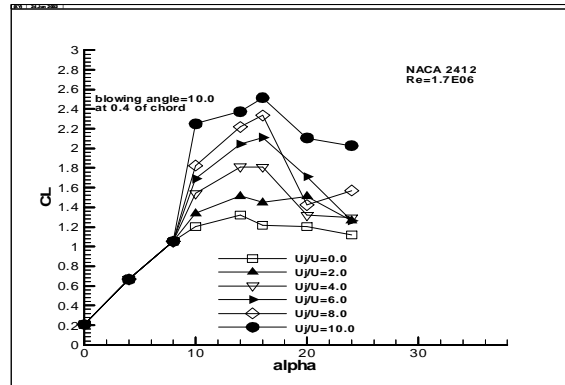


Figure (8) Lift coefficient vs. alpha at blowing position (0.4C)

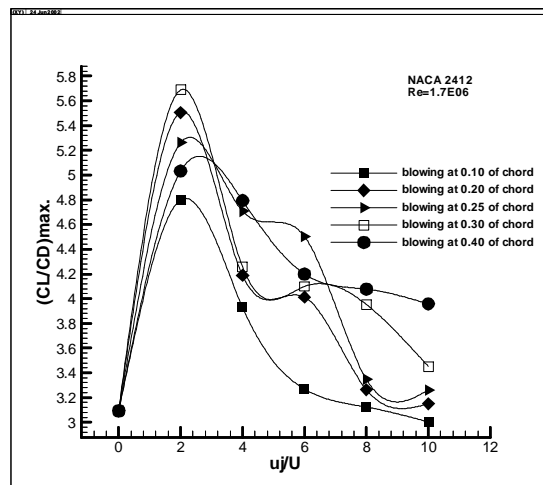


Figure (9) $(C_l/C_d)_{max}$ Vs. U_j/U at $Re=1.7*10$

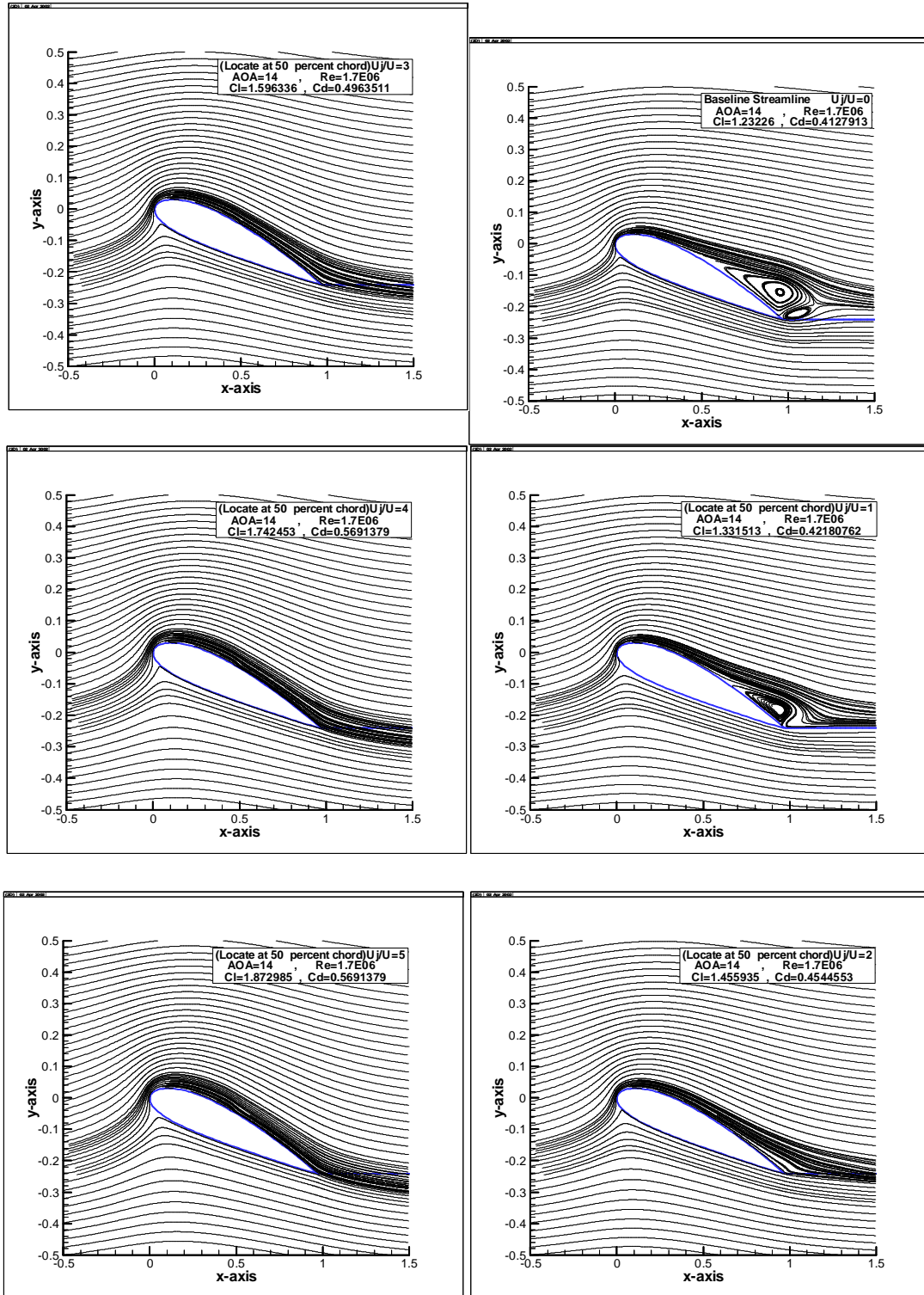


Figure (10) Stream lines and effect of blowing at 50% chord with different jet blowing